Output Feedback Dynamic Surface Control of Flexible-Joint Robots

Sung Jin Yoo, Jin Bae Park*, and Yoon Ho Choi

Abstract: A new output feedback controller design approach for flexible-joint (FJ) robots via the observer dynamic surface design technique is presented. The proposed approach only requires the feedback of position states. We first design an observer to estimate the link and actuator velocity information. Then, the link position tracking controller using the observer dynamic surface design procedure is developed. Therefore, the proposed controller can be simpler than the observer backstepping controller. From the Lyapunov stability analysis, it is shown that all signals in a closed-loop system are uniformly ultimately bounded. Finally, the simulation results of a three-link FJ robot are presented to validate the good position tracking performance of the proposed control system.

Keywords: Dynamic surface control, flexible-joint robots, output feedback.

---

1. INTRODUCTION

During the past few years, significant research efforts have been devoted to solve the tracking control problem for the flexible-joint (FJ) robots [1-7]. One of the problems that has prevented the application of these controllers is that the knowledge of four state variables is required. However, velocity measurement devices such as tachometers are easily contaminated with noise and are frequently omitted due to the savings in cost, volume, and weight. Therefore, many researchers proposed observers to estimate the states of FJ robots, and the output feedback methods using them. Tomei [8] presented the state observer for FJ robots with the link position and velocity. In [9], the nonlinear observer for FJ robots with only position measurements was designed. Abdollahi *et al.* [10] proposed the stable neural network observer for multivariable nonlinear systems and applied it to FJ robots. In [11], the output tracking controller for FJ robots was presented based on a two-time scale sliding-mode technique and a high gain estimator. Angeles and Nijmeijer [12] proposed an observer-based synchronization controller for FJ robots which are interconnected in a master-slave scheme. In [13], Jankovic presented an approach to control FJ robots using only the position and velocity measurements on the actuator.

The backstepping technique [14], in particular, has been widely used to design output feedback controllers for FJ robots. Nicosia and Tomei [15] developed a global dynamic output feedback backstepping controller for FJ robots using only the measurements of the link position and speed. In addition, they proposed a backstepping control method for FJ robots with only link position feedback [16]. Oh and Lee [17] presented a tracking controller using a backstepping design approach for FJ robots with only position measurements. In [18], an adaptive partial state feedback controller for FJ robots without velocity measurements was designed via an integrator backstepping procedure. Dixon *et al.* [19] suggested the global adaptive partial state feedback tracking controller for FJ robots using the backstepping technique. However, the backstepping algorithm has the "explosion of complexity" problem which is caused by the repeated differentiations of virtual controllers [20,21]. To overcome this problem, Swaroop *et al.* proposed a dynamic surface control (DSC) technique adding a first-order low-pass filter at each step of the backstepping design procedure. In addition, this idea was extended to adaptive systems to treat parametric nonlinear functions [21] and uncertain nonlinear functions [22]. Besides, Song and Hedrick [23] suggested an output feedback DSC (OFDSC) method using a convex optimization technique for nonlinear systems. However, these works only used DSC technique to control single-input-single-output systems.

Recently, we suggested the full state feedback

Manuscript received March 27, 2007; accepted February 1, 2008. Recommended by Editorial Board member Young Il Lee under the direction of Editor Jae-Bok Song. This work was supported in part by Yonsei University Institute of TMS Information Technology, a Brain Korea 21 program and in part by MOCIE through EIRC program with Yonsei Electric Power Research Center (YEPRC) at Yonsei University, Seoul, Korea.

Sung Jin Yoo and Jin Bae Park are with the Department of Electrical and Electronic Engineering, Yonsei University, Seodaemun-Gu, Seoul 120-749, Korea (e-mails: {niceguy 1201, jbpark}@yonsei.ac.kr).

Yoon Ho Choi is with the School of Electronic Engineering, Kyonggi University, Suwon, Kyonggi-Do 443-760, Korea (e-mail: yhchoi@kyonggi.ac.kr).

* Corresponding author.

control approach using the DSC technique for FJ robots which are multi-input-multi-output systems [24]. In this paper, we present the output feedback control approach for FJ robots via the observer dynamic surface design technique. For the OFDSC system design, we first introduce an observer for the FJ robot model to estimate the link and actuator velocity information. Then, the control law using the state estimates is induced from the DSC design procedure. This design procedure comparable to the observer backstepping is called the observer DSC technique. From the Lyapunov stability analysis, it is shown that all signals in a closed-loop system are uniformly ultimately bounded. Finally, we simulate the three-link FJ manipulator with complex nonlinear functions to show the effectiveness of the proposed OFDSC scheme.

This paper is organized as follows. In Section 2, we introduce the dynamic model of FJ robot systems. In Section 3, the observer is presented to estimate the link and actuator velocity. In addition, the OFDSC law is proposed based on the designed observer. Besides, the stability and performance of the proposed OFDSC system are analyzed based on Lyapunov stability theorem. Simulation results are discussed in Section 4 Section 5 gives some conclusions.

2. DYNAMICS OF FJ ROBOTS

The dynamic model of an n-link FJ robot composed of robot dynamics and actuator dynamics can be described by [25]:

$$\mathbf{M}(\mathbf{q})\ddot{\mathbf{q}} + \mathbf{C}(\mathbf{q},\dot{\mathbf{q}})\dot{\mathbf{q}} + \mathbf{G}(\mathbf{q}) + \mathbf{F}\dot{\mathbf{q}} + \mathbf{K_m}(\mathbf{q} - \mathbf{q_m}) = 0, \tag{1}$$

$$\mathbf{J}\ddot{\mathbf{q}}_\mathbf{m} + \mathbf{B}\dot{\mathbf{q}}_\mathbf{m} + \mathbf{K_m}(\mathbf{q_m} - \mathbf{q}) = \mathbf{u}, \tag{2}$$

where $\mathbf{q}$, $\dot{\mathbf{q}}$, $\ddot{\mathbf{q}} \in R^n$ denote the link position, velocity, and acceleration vectors, respectively. $\mathbf{M}(\mathbf{q}) \in R^{n\times n}$ is the inertia matrix, $\mathbf{C}(\mathbf{q},\dot{\mathbf{q}}) \in R^{n\times n}$ denotes the Coriolis-centripetal matrix, $\mathbf{G}(\mathbf{q}) \in R^n$ is the gravity vector, and $\mathbf{F} \in R^{n\times n}$ is a diagonal, positive definite matrix representing the coefficient of friction at each joint. $\mathbf{q_m}$, $\dot{\mathbf{q}}_\mathbf{m}$, $\ddot{\mathbf{q}}_\mathbf{m} \in R^n$ denote the actuator position, velocity, and acceleration vectors, respectively. The constant positive definite, diagonal matrices $\mathbf{K_m} \in R^{n\times n}$, $\mathbf{J} \in R^{n\times n}$, and $\mathbf{B} \in R^{n\times n}$ represent the joint flexibility, the actuator inertia, and the natural damping term, respectively. The control vector $\mathbf{u} \in R^n$ is used as the torque input at each actuator.

Property 1 [17]: The link inertia matrix $\mathbf{M}(\mathbf{q})$ is symmetric, positive definite matrix which satisfies $M_m \le \|\mathbf{M}(\mathbf{q})\|_2 \le M_M$ where $\|\cdot\|_2$ denotes the matrix induced two-norm and M_m, M_M are positive constants. In addition, $\mathbf{M}^{-1}(\mathbf{q})$ is uniformly bounded.

Property 2: The Coriolis-centripetal matrix $\mathbf{C}(\mathbf{q}, \dot{\mathbf{q}})$ can be defined such that the matrix $\dot{\mathbf{M}}(\mathbf{q}) - 2\mathbf{C}(\mathbf{q},\dot{\mathbf{q}})$ is the skew-symmetric matrix, and satisfies $\mathbf{C}(\mathbf{q},\xi)\zeta = \mathbf{C}(\mathbf{q},\zeta)\xi$ where ξ, $\zeta \in R^n$ are any vectors.

Property 3: The Coriolis-centripetal matrix $\mathbf{C}(\mathbf{q}, \dot{\mathbf{q}})$ is upper bounded, that is $\|\mathbf{C}(\mathbf{q},\dot{\mathbf{q}})\|_2 \le C_M \|\dot{\mathbf{q}}\|$ where C_M is a known positive constant.

Property 4: $\|\mathbf{M}^{-1}(\mathbf{q})\mathbf{K_m}\|_2 \le H_M$ where H_M is a known positive constant.

Property 4 is reasonable due to Property 1 and a constant positive definite matrix $\mathbf{K_m}$.

Assumption 1: The system states $\mathbf{q}$ and $\mathbf{q_m}$ are only available for feedback, that is, the outputs of the FJ robot system are $\mathbf{q}$ and $\mathbf{q_m}$.

Assumption 2: The desired trajectory vector $\mathbf{q_d}$, its first and second derivatives $\mathbf{q_d^{(1)}}$, $\mathbf{q_d^{(2)}}$ are only available, and bounded where $\mathbf{q_d^{(i)}}$ denotes the ith derivative of $\mathbf{q_d}$.

Assumption 3: The link velocity $\dot{\mathbf{q}}$ is bounded as $\|\dot{\mathbf{q}}\| < \omega_1$ where ω_1 is a known positive constant.

Assumption 2 indicates that our controller via the dynamic surface design technique does not requires $\mathbf{q_d^{(3)}}$ and $\mathbf{q_d^{(4)}}$ compared with the controller via the backstepping technique [15-19]. In Assumption 3, ω_1 does not mean a tight upper bound for $\|\dot{\mathbf{q}}\|$, that is, any upper bound does. Reasonable bounds can be obtained from manufacturer's specification and structural limitations of the robot [12,13]. As a preliminary to the output feedback controller design, if we define the state space variables as $\mathbf{x}_1 = \mathbf{q}$, $\mathbf{x}_2 = \dot{\mathbf{q}}$, $\mathbf{x}_3 = \mathbf{q_m}$, and $\mathbf{x}_4 = \dot{\mathbf{q}}_\mathbf{m}$, the FJ robot system is described as follows:

$$\dot{\mathbf{x}}_1 = \mathbf{x}_2, \tag{3}$$

$$\mathbf{M}(\mathbf{x}_1)\dot{\mathbf{x}} = -\mathbf{C}(\mathbf{x}_1,\mathbf{x}_2)\mathbf{x}_2 - \mathbf{G}(\mathbf{x}_1) - \mathbf{F}\mathbf{x}_2 - \mathbf{K_m}(\mathbf{x}_1 - \mathbf{x}_3), \tag{4}$$

$$\dot{\mathbf{x}}_3 = \mathbf{x}_4, \tag{5}$$

$$\dot{\mathbf{x}}_4 = \mathbf{J}^{-1}[-\mathbf{B}\mathbf{x}_4 - \mathbf{K_m}(\mathbf{x}_3 - \mathbf{x}_1) + \mathbf{u}]. \tag{6}$$

3. OFDSC SYSTEM FOR FJ ROBOTS

In this section, we first introduce the observer to estimate the link and actuator velocity information of the FJ robots. Then, the OFDSC system for FJ robots is designed. Finally, the stability of the designed output feedback system is analyzed.

3.1. Observer design for FJ robots

Define the estimates $\hat{\mathbf{x}}_\chi$ of the states $\mathbf{x}_\chi$ ($\chi=1,\ldots,4$) as follows:

$$\hat{\mathbf{x}}_1=\mathbf{z}_1, \quad (7)$$

$$\hat{\mathbf{x}}_2=\mathbf{z}_2+l_1(\mathbf{x}_1-\mathbf{z}_1), \quad (8)$$

$$\hat{\mathbf{x}}_3=\mathbf{z}_3, \quad (9)$$

$$\hat{\mathbf{x}}_4=\mathbf{z}_4+l_2(\mathbf{x}_3-\mathbf{z}_3), \quad (10)$$

where l_1, l_2 are design parameters, and $\mathbf{z}_\chi$ denote observer states. The observer for FJ robots is presented in the following form:

$$\dot{\mathbf{z}}_1=\mathbf{z}_2+l_1(\mathbf{x}_1-\mathbf{z}_1)+\mathbf{D}_1(\mathbf{x}_1-\mathbf{z}_1), \quad (11)$$

$$\begin{aligned}\mathbf{M}(\mathbf{x}_1)\dot{\mathbf{z}}_2=&-\mathbf{C}(\mathbf{x}_1,\mathbf{z}_2+l_1(\mathbf{x}_1-\mathbf{z}_1))(\mathbf{z}_2+l_1(\mathbf{x}_1-\mathbf{z}_1))\\&-\mathbf{G}(\mathbf{x}_1)-\mathbf{F}(\mathbf{z}_2+l_1(\mathbf{x}_1-\mathbf{z}_1))\\&-\mathbf{K_m}(\mathbf{x}_1-\mathbf{x}_3)+\overline{\mathbf{D}}_2(\mathbf{x}_1-\mathbf{z}_1),\end{aligned} \quad (12)$$

$$\dot{\mathbf{z}}_3=\mathbf{z}_4+l_2(\mathbf{x}_3-\mathbf{z}_3)+\mathbf{D}_3(\mathbf{x}_3-\mathbf{z}_3), \quad (13)$$

$$\begin{aligned}\dot{\mathbf{z}}_4=&\mathbf{J}^{-1}[-\mathbf{B}(\mathbf{z}_4+l_2(\mathbf{x}_3-\mathbf{z}_3))+\mathbf{u}\\&-\mathbf{K_m}(\mathbf{x}_3-\mathbf{x}_1)]+\overline{\mathbf{D}}_4(\mathbf{x}_3-\mathbf{z}_3),\end{aligned} \quad (14)$$

where $\mathbf{D}_1$, $\overline{\mathbf{D}}_2$, $\mathbf{D}_3$, and $\overline{\mathbf{D}}_4$ are the observer gain matrices to be designed later, and the outputs $\mathbf{x}_1$, $\mathbf{x}_3$ and the input $\mathbf{u}$ of the FJ robots are used as the inputs of the observer system. Then, to consider the observation error dynamics, we can rewrite the observer dynamics (11)-(14) using the estimate variables (7)-(10) as follows:

$$\dot{\hat{\mathbf{x}}}_1=\hat{\mathbf{x}}_2+\mathbf{D}_1\tilde{\mathbf{x}}_1, \quad (15)$$

$$\begin{aligned}\mathbf{M}(\mathbf{x}_1)\dot{\hat{\mathbf{x}}}_2=&-\mathbf{C}(\mathbf{x}_1,\hat{\mathbf{x}}_2)\hat{\mathbf{x}}_2-\mathbf{G}(\mathbf{x}_1)-\mathbf{F}\hat{\mathbf{x}}_2\\&-\mathbf{K_m}(\mathbf{x}_1-\mathbf{x}_3)+l_1\mathbf{M}(\mathbf{x}_1)\tilde{\mathbf{x}}_2+\mathbf{D}_2\tilde{\mathbf{x}}_1,\end{aligned} \quad (16)$$

$$\dot{\hat{\mathbf{x}}}_3=\hat{\mathbf{x}}_4+\mathbf{D}_3\tilde{\mathbf{x}}_3, \quad (17)$$

$$\begin{aligned}\dot{\hat{\mathbf{x}}}_4=&\mathbf{J}^{-1}[-\mathbf{B}\hat{\mathbf{x}}_4-\mathbf{K_m}(\mathbf{x}_3-\mathbf{x}_1)+\mathbf{u}]\\&+l_2\tilde{\mathbf{x}}_4+\mathbf{D}_4\tilde{\mathbf{x}}_3,\end{aligned} \quad (18)$$

where $\tilde{\mathbf{x}}_\chi=\mathbf{x}_\chi-\hat{\mathbf{x}}_\chi$ ($\chi=1,\ldots,4$) denote the observation errors and $\mathbf{D}_2=\overline{\mathbf{D}}_2-l_1\mathbf{M}(\mathbf{x}_1)\mathbf{D}_1$ and $\mathbf{D}_4=\overline{\mathbf{D}}_4-l_2\mathbf{D}_3$ are the new observer gain matrices.

Remark 1: The observer dynamics (15)-(18) cannot be implemented due to the unknown states $\mathbf{x}_2$, $\mathbf{x}_4$. Therefore, in this paper, we use the observer dynamics (7)-(14) based on only the known states $\mathbf{x}_1$, $\mathbf{x}_3$ to implement the observer for FJ robots.

3.2. Output feedback controller design for FJ robots

The control objective is to design an output feedback control system for the state vector $\mathbf{x}_1$ to track the desired trajectory vector $\mathbf{q_d}$. In our controller design procedure, the true velocities of the FJ robots are replaced by the estimated states $\hat{\mathbf{x}}_2$ and $\hat{\mathbf{x}}_4$. We now design step by step the output feedback control system via the observer DSC technique.

Step 1: Design the virtual control law for $\hat{\mathbf{x}}_2$. The first error surface vector is defined as $\mathbf{S}_1=\mathbf{x}_1-\mathbf{q_d}$, and its derivative is

$$\begin{aligned}\dot{\mathbf{S}}_1&=\mathbf{x}_2-\dot{\mathbf{q}}_\mathbf{d}\\&=\hat{\mathbf{x}}_2+\tilde{\mathbf{x}}_2-\dot{\mathbf{q}}_\mathbf{d}.\end{aligned} \quad (19)$$

Choose a virtual control vector $\overline{\mathbf{x}}_2$ as follows:

$$\overline{\mathbf{x}}_2=-k_1\mathbf{S}_1+\dot{\mathbf{q}}_\mathbf{d}, \quad (20)$$

where k_1 is a positive constant. Then, to obtain the filtering virtual control vector $\mathbf{x}_{2\mathbf{f}}$, we pass $\overline{\mathbf{x}}_2$ through a first-order filter with a time constant $\tau_2>0$ as follows:

$$\tau_2\dot{\mathbf{x}}_{2\mathbf{f}}+\mathbf{x}_{2\mathbf{f}}=\overline{\mathbf{x}}_2,\quad \mathbf{x}_{2\mathbf{f}}(0)=\overline{\mathbf{x}}_2(0). \quad (21)$$

Step 2: Design the virtual control law for $\mathbf{x}_3$. Define the second error surface, with the filtering virtual control vector $\mathbf{x}_{2\mathbf{f}}$, as

$$\mathbf{S}_2=\hat{\mathbf{x}}_2-\mathbf{x}_{2\mathbf{f}}. \quad (22)$$

Then, differentiating (22) and substituting (16) yields

$$\begin{aligned}\dot{\mathbf{S}}_2&=\dot{\hat{\mathbf{x}}}_2-\dot{\mathbf{x}}_{2\mathbf{f}}\\&=\mathbf{M}^{-1}(\mathbf{x}_1)[-\mathbf{C}(\mathbf{x}_1,\hat{\mathbf{x}}_2)\hat{\mathbf{x}}_2-\mathbf{G}(\mathbf{x}_1)-\mathbf{F}\hat{\mathbf{x}}_2\\&\quad-\mathbf{K_m}(\mathbf{x}_1-\mathbf{x}_3)+\mathbf{D}_2\tilde{\mathbf{x}}_1]+l_1\tilde{\mathbf{x}}_2-\dot{\mathbf{x}}_{2\mathbf{f}}.\end{aligned} \quad (23)$$

Choose a virtual control vector $\overline{\mathbf{x}}_3$ using (21) as follows:

$$\begin{aligned}\overline{\mathbf{x}}_3=\mathbf{K_m}^{-1}\Bigg[&\mathbf{K_m}\mathbf{x}_1+\mathbf{C}(\mathbf{x}_1,\hat{\mathbf{x}}_2)\hat{\mathbf{x}}_2+\mathbf{G}(\mathbf{x}_1)+\mathbf{F}\hat{\mathbf{x}}_2\\&-\mathbf{D}_2\tilde{\mathbf{x}}_1+\mathbf{M}(\mathbf{x}_1)\left\{-k_2\mathbf{S}_2+\frac{\overline{\mathbf{x}}_2-\mathbf{x}_{2\mathbf{f}}}{\tau_2}\right\}\Bigg],\end{aligned} \quad (24)$$

where $k_2>0$ is a design parameter. Then, we pass $\overline{\mathbf{x}}_3$ through the second first-order filter to obtain $\mathbf{x}_{3\mathbf{f}}$ as follows:

$$\tau_3\dot{\mathbf{x}}_{3\mathbf{f}}+\mathbf{x}_{3\mathbf{f}}=\overline{\mathbf{x}}_3,\quad \mathbf{x}_{3\mathbf{f}}(0)=\overline{\mathbf{x}}_3(0), \quad (25)$$

where τ_3 is a small positive design parameter, that is, a time constant.

Step 3: Design the virtual control law for $\hat{\mathbf{x}}_4$.

Define the third error surface, with the filtering virtual control vector $\mathbf{x}_{3f}$, as

$$\mathbf{S}_3 = \mathbf{x}_3 - \mathbf{x}_{3f} \tag{26}$$

and its derivative is

$$\begin{aligned}\dot{\mathbf{S}}_3 &= \mathbf{x}_4 - \dot{\mathbf{x}}_{3f} \\ &= \hat{\mathbf{x}}_4 + \tilde{\mathbf{x}}_4 - \dot{\mathbf{x}}_{3f}.\end{aligned} \tag{27}$$

Choose a virtual control vector $\overline{\mathbf{x}}_4$ using (25) as follows:

$$\overline{\mathbf{x}}_4 = -k_3\mathbf{S}_3 + \frac{\overline{\mathbf{x}}_3 - \mathbf{x}_{3f}}{\tau_3}, \tag{28}$$

where k_3 is a positive constant. Then, we pass $\overline{\mathbf{x}}_4$ through the third first-order filter with a time constant $\tau_4 > 0$ to obtain $\mathbf{x}_{4f}$ as follows:

$$\tau_4\dot{\mathbf{x}}_{4f} + \mathbf{x}_{4f} = \overline{\mathbf{x}}_4, \quad \mathbf{x}_{4f}(0) = \overline{\mathbf{x}}_4(0). \tag{29}$$

Step 4: Design the actual control vector $\mathbf{u}$. Define the fourth error surface, with the filtering virtual control vector $\mathbf{x}_{4f}$, as

$$\mathbf{S}_4 = \hat{\mathbf{x}}_4 - \mathbf{x}_{4f} \tag{30}$$

and its derivative is

$$\begin{aligned}\dot{\mathbf{S}}_4 &= \dot{\hat{\mathbf{x}}}_4 - \dot{\mathbf{x}}_{4f} \\ &= \mathbf{J}^{-1}[-\mathbf{B}\hat{\mathbf{x}}_4 - \mathbf{K}_m(\mathbf{x}_3 - \mathbf{x}_1) + \mathbf{u}] \\ &\quad + l_2\tilde{\mathbf{x}}_4 + \mathbf{D}_4\tilde{\mathbf{x}}_3 - \dot{\mathbf{x}}_{4f}.\end{aligned} \tag{31}$$

Choose an actual control vector $\mathbf{u}$ using (29) as follows:

$$\begin{aligned}\mathbf{u} &= \mathbf{B}\hat{\mathbf{x}}_4 + \mathbf{K}_m(\mathbf{x}_3 - \mathbf{x}_1) \\ &\quad + \mathbf{J}[-k_4\mathbf{S}_4 - \mathbf{D}_4\tilde{\mathbf{x}}_3 + \frac{\overline{\mathbf{x}}_4 - \mathbf{x}_{4f}}{\tau_4}],\end{aligned} \tag{32}$$

where k_4 is a positive constant.

Remark 2: Compared with the previous works [15-17] using the backstepping technique for FJ robots, the proposed control method does not require the repeated derivatives of the virtual controllers because they are computed easily by the first order filter (i.e., $\dot{\mathbf{x}}_{jf} = (\overline{\mathbf{x}}_j - \mathbf{x}_{jf})/\tau_j$, $j = 2,3,4$). Thus, the proposed control system can be designed more simply than the backstepping control systems [15-17].

3.3. Stability analysis

In this section, we now show that all signals of the proposed OFDSC system are uniformly ultimately bounded. For the stability analysis, we define analytic expressions of the closed-loop system via observation errors ($\tilde{\mathbf{x}}_1$, $\tilde{\mathbf{x}}_2$, $\tilde{\mathbf{x}}_3$, and $\tilde{\mathbf{x}}_4$), surface errors ($\mathbf{S}_1$, $\mathbf{S}_2$, $\mathbf{S}_3$, and $\mathbf{S}_4$), and boundary layer errors ($\mathbf{y}_2$, $\mathbf{y}_3$, and $\mathbf{y}_4$).

From (3)-(6) and (15)-(18), we first obtain the observation error dynamics as follows:

$$\dot{\tilde{\mathbf{x}}}_1 = \tilde{\mathbf{x}}_2 - \mathbf{D}_1\tilde{\mathbf{x}}_1, \tag{33}$$

$$\begin{aligned}\mathbf{M}(\mathbf{x}_1)\dot{\tilde{\mathbf{x}}}_2 &= -\mathbf{C}(\mathbf{x}_1,\mathbf{x}_2)\mathbf{x}_2 + \mathbf{C}(\mathbf{x}_1,\hat{\mathbf{x}}_2)\hat{\mathbf{x}}_2 - \mathbf{F}\tilde{\mathbf{x}}_2 \\ &\quad - l_1\mathbf{M}(\mathbf{x}_1)\tilde{\mathbf{x}}_2 - \mathbf{D}_2\tilde{\mathbf{x}}_1,\end{aligned} \tag{34}$$

$$\dot{\tilde{\mathbf{x}}}_3 = \tilde{\mathbf{x}}_4 - \mathbf{D}_3\tilde{\mathbf{x}}_3, \tag{35}$$

$$\dot{\tilde{\mathbf{x}}}_4 = -\mathbf{J}^{-1}\mathbf{B}\tilde{\mathbf{x}}_4 - l_2\tilde{\mathbf{x}}_4 - \mathbf{D}_4\tilde{\mathbf{x}}_3. \tag{36}$$

By using Property 2, adding and subtracting $\mathbf{C}(\mathbf{x}_1,\mathbf{x}_2)\hat{\mathbf{x}}_2$, the observation error dynamics (34) can be rewritten by

$$\begin{aligned}\mathbf{M}(\mathbf{x}_1)\dot{\tilde{\mathbf{x}}}_2 &= -\mathbf{C}(\mathbf{x}_1,\mathbf{x}_2)\tilde{\mathbf{x}}_2 - \mathbf{C}(\mathbf{x}_1,\hat{\mathbf{x}}_2)\tilde{\mathbf{x}}_2 - \mathbf{F}\tilde{\mathbf{x}}_2 \\ &\quad - l_1\mathbf{M}(\mathbf{x}_1)\tilde{\mathbf{x}}_2 - \mathbf{D}_2\tilde{\mathbf{x}}_1.\end{aligned} \tag{37}$$

Then, we describe the derivative of the surface errors as follows:

$$\dot{\mathbf{S}}_1 = \mathbf{S}_2 + \mathbf{x}_{2f} + \tilde{\mathbf{x}}_2 - \dot{\mathbf{q}}_d, \tag{38}$$

$$\begin{aligned}\dot{\mathbf{S}}_2 &= \mathbf{M}^{-1}(\mathbf{x}_1)[-\mathbf{C}(\mathbf{x}_1,\hat{\mathbf{x}}_2)\hat{\mathbf{x}}_2 - \mathbf{G}(\mathbf{x}_1) \\ &\quad - \mathbf{F}\hat{\mathbf{x}}_2 - \mathbf{K}_m\mathbf{x}_1 + \mathbf{K}_m(\mathbf{S}_3 + \mathbf{x}_{3f}) \\ &\quad + \mathbf{D}_2\tilde{\mathbf{x}}_1] + l_1\tilde{\mathbf{x}}_2 - \dot{\mathbf{x}}_{2f},\end{aligned} \tag{39}$$

$$\dot{\mathbf{S}}_3 = \mathbf{S}_4 + \mathbf{x}_{4f} + \tilde{\mathbf{x}}_4 - \dot{\mathbf{x}}_{3f}, \tag{40}$$

$$\dot{\mathbf{S}}_4 = -k_4\mathbf{S}_4 + l_2\tilde{\mathbf{x}}_4. \tag{41}$$

Define the boundary layer errors as

$$\begin{aligned}\mathbf{y}_2 &= \mathbf{x}_{2f} - \overline{\mathbf{x}}_2 \\ &= k_1\mathbf{S}_1 - \dot{\mathbf{q}}_d + \mathbf{x}_{2f},\end{aligned} \tag{42}$$

$$\begin{aligned}\mathbf{y}_3 &= \mathbf{x}_{3f} - \overline{\mathbf{x}}_3 \\ &= -\mathbf{K}_m^{-1}\Big[\mathbf{K}_m\mathbf{x}_1 + \mathbf{C}(\mathbf{x}_1,\hat{\mathbf{x}}_2)\hat{\mathbf{x}}_2 + \mathbf{G}(\mathbf{x}_1) + \mathbf{F}\hat{\mathbf{x}}_2 \\ &\quad -\mathbf{D}_2\tilde{\mathbf{x}}_1 + \mathbf{M}(\mathbf{x}_1)\Big\{-k_2\mathbf{S}_2 - \frac{\mathbf{y}_2}{\tau_2}\Big\}\Big] + \mathbf{x}_{3f},\end{aligned} \tag{43}$$

$$\mathbf{y}_4 = \mathbf{x}_{4f} - \overline{\mathbf{x}}_4 = k_3\mathbf{S}_3 + \frac{\mathbf{y}_3}{\tau_3} + \mathbf{x}_{4f}. \tag{44}$$

From the boundary layer errors (42)-(44), (38)-(41) can be expressed by

$$\dot{\mathbf{S}}_1 = \mathbf{S}_2 + \mathbf{y}_2 - k_1\mathbf{S}_1 + \tilde{\mathbf{x}}_2, \tag{45}$$

$$\dot{\mathbf{S}}_2 = \mathbf{M}^{-1}(\mathbf{x}_1)\mathbf{K}_m(\mathbf{S}_3 + \mathbf{y}_3) - k_2\mathbf{S}_2 + l_1\tilde{\mathbf{x}}_2, \tag{46}$$

$$\dot{\mathbf{S}}_3 = \mathbf{S}_4 + \mathbf{y}_4 - k_3\mathbf{S}_3 + \tilde{\mathbf{x}}_4, \tag{47}$$

$$\dot{\mathbf{S}}_4 = -k_4\mathbf{S}_4 + l_2\tilde{\mathbf{x}}_4. \tag{48}$$

Differentiating (42)-(44), we can obtain

Table 1. Simulation parameters for the robot dynamics.

	Mass (m_i Kg)	Link (l_i, m)	Moment of Inertia (I_i, Kgm^2)
Joint 1	1.0	0.5	43.33×10^{-3}
Joint 2	0.7	0.4	25.08×10^{-3}
Joint 3	1.4	0.3	32.67×10^{-3}

$$\dot{\mathbf{y}}_2 = -\frac{\mathbf{y}_2}{\tau_2} + \Omega_2(\mathbf{S}_1,\mathbf{S}_2,\mathbf{y}_2,\tilde{\mathbf{x}}_2,\mathbf{Q_d}), \quad (49)$$

$$\dot{\mathbf{y}}_3 = -\frac{\mathbf{y}_3}{\tau_3} + \Omega_3(\mathbf{S}_1,\ldots,\mathbf{S}_3,\mathbf{y}_2,\mathbf{y}_3,\tilde{\mathbf{x}}_1,\ldots,\tilde{\mathbf{x}}_4,\mathbf{Q_d}), \quad (50)$$

$$\dot{\mathbf{y}}_4 = -\frac{\mathbf{y}_4}{\tau_4} + \Omega_4(\mathbf{S}_1,\ldots,\mathbf{S}_4,\mathbf{y}_2,\mathbf{y}_3,\mathbf{y}_4,\tilde{\mathbf{x}}_1,\ldots,\tilde{\mathbf{x}}_4,\mathbf{Q_d}), \quad (51)$$

where $\mathbf{Q_d} = [\mathbf{q_d^T}, \dot{\mathbf{q}}_\mathbf{d}^\mathbf{T}, \ddot{\mathbf{q}}_\mathbf{d}^\mathbf{T}]^\mathrm{T}$,

$$\begin{aligned}
&\Omega_2(\mathbf{S}_1,\mathbf{S}_2,\mathbf{y}_2,\tilde{\mathbf{x}}_2,\mathbf{Q_d}) \\
&= \mathbf{k}_1\dot{\mathbf{S}}_1 - \ddot{\mathbf{q}}_\mathbf{d}, \Omega_3(\mathbf{S}_1,\ldots,\mathbf{S}_3,\mathbf{y}_2,\mathbf{y}_3,\tilde{\mathbf{x}}_1,\ldots,\tilde{\mathbf{x}}_4,\mathbf{Q_d}) \\
&= -\mathbf{K_m^{-1}}[\mathbf{K_m}\dot{\mathbf{x}}_1 + (\dot{\mathbf{x}}_1^\mathrm{T}\frac{\partial \mathbf{C}}{\partial \mathbf{x}_1} + \dot{\hat{\mathbf{x}}}_2^\mathrm{T}\frac{\partial \mathbf{C}}{\partial \hat{\mathbf{x}}_2})\hat{\mathbf{x}}_2 + \mathbf{C}\dot{\hat{\mathbf{x}}}_2 \\
&\quad + \frac{\partial \mathbf{G}}{\partial \mathbf{x}_1}\dot{\mathbf{x}}_1 + \mathbf{F}\dot{\hat{\mathbf{x}}}_2 - \mathbf{D}_2\dot{\tilde{\mathbf{x}}}_1 + \dot{\mathbf{x}}_1^\mathrm{T}\frac{\partial \mathbf{M}}{\partial \mathbf{x}_1}\{-k_2\mathbf{S}_2 - \frac{\mathbf{y}_2}{\tau_2}\} \\
&\quad + \mathbf{M}\{-k_2\dot{\mathbf{S}}_2 - \frac{\dot{\mathbf{y}}_2}{\tau_2}\}],
\end{aligned}$$

and

$$\Omega_4(\mathbf{S}_1,\ldots,\mathbf{S}_4,\mathbf{y}_2,\mathbf{y}_3,\mathbf{y}_4,\tilde{\mathbf{x}}_1,\ldots,\tilde{\mathbf{x}}_4,\mathbf{Q_d}) = k_3\dot{\mathbf{S}}_3 + \frac{\dot{\mathbf{y}}_3}{\tau_3}$$

are the continuous functions.

Theorem 1: Suppose that the dynamics (3)-(6) of the FJ robots is observed by the observer (7)-(14), and is controlled by the proposed controller (32). If the proposed output feedback control system satisfies Assumptions 1-3, then for any initial conditions satisfying $V(0) \le p$ where p is any positive constant, there exist k_j, l_1, l_2, $\mathbf{D}_j$, τ_h ($j = 1,\ldots,4$, $h = 2,3,4$) such that all signals of the closed-loop system are uniformly ultimately bounded. In addition, all errors in the closed-loop system may be kept arbitrarily small by adjusting the design parameters.

Proof: See Appendix I.

Remark 3: The proposed output feedback control scheme for FJ robots can be summarized by the observer ((7)-(14)) and the DSC system ((20), (21), (24), (25), (28), (29), and (32)). Accordingly, our control system can be designed more easily and simply than the output feedback control system via the backstepping technique.

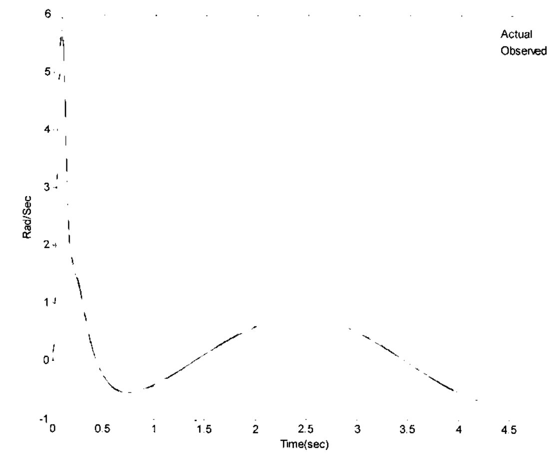

(a) Joint 1.

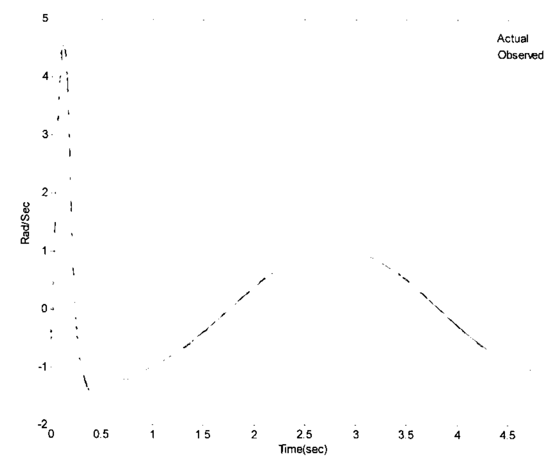

(b) Joint 2.

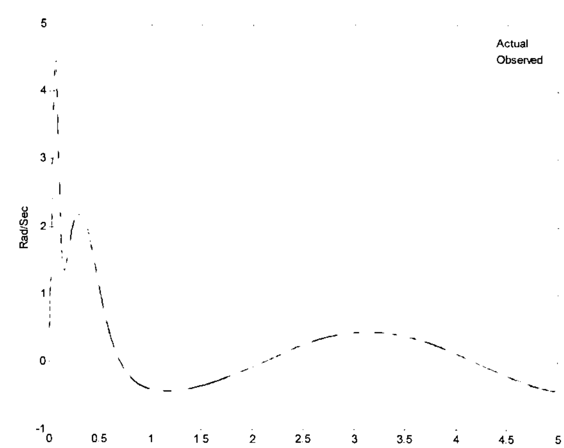

(c) Joint 3.

Fig. 1. Observation results of the state $\mathbf{x}_2$ for the three-link FJ manipulator.

4. SIMULATION RESULTS

In this simulation, we consider a three-link FJ manipulator to validate the effectiveness of the proposed OFDSC system.

Remark 4: We do not compare the proposed control method with the backstepping-based control

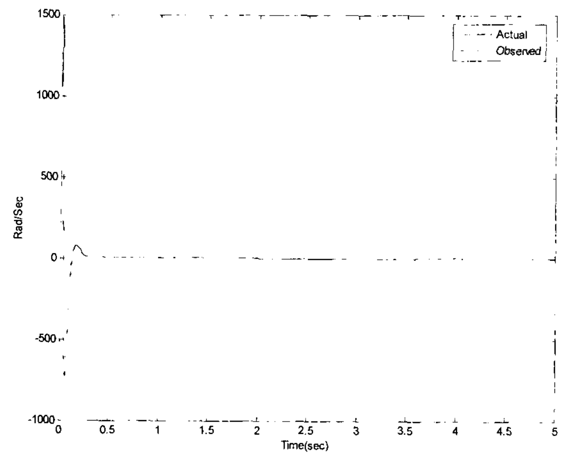

(a) Joint 1.

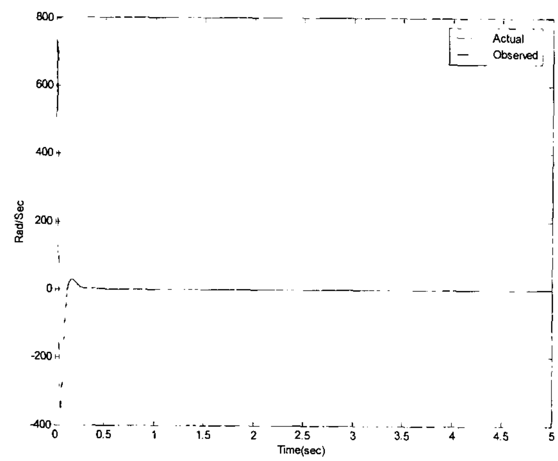

(b) Joint 2.

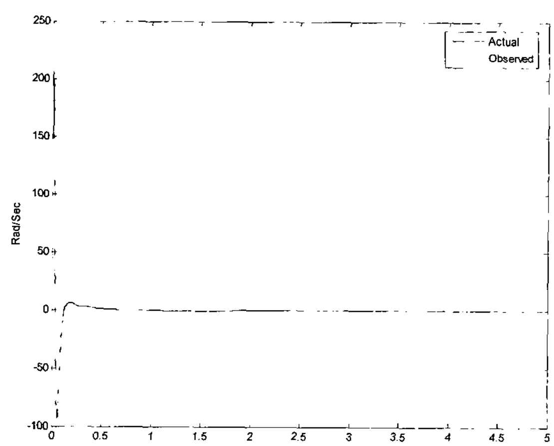

(c) Joint 3.

Fig. 2. Observation results of the state $\mathbf{x}_4$ for the three-link FJ manipulator.

methods [15-17] since the performance of the DSC system is similar to that of the backstepping control system [20]. That is, this simulation focuses on the simplicity of the controller design method for the n-link FJ robots with the complex nonlinearity. Therefore, we consider a three-link FJ manipulator, not an one-link or a two-link FJ manipulator.

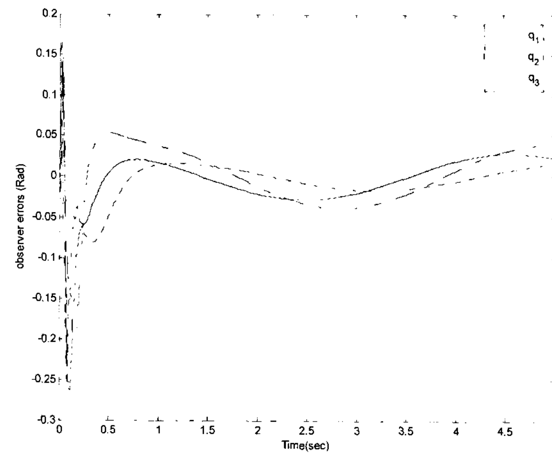

(a) State $\mathbf{x}_2$.

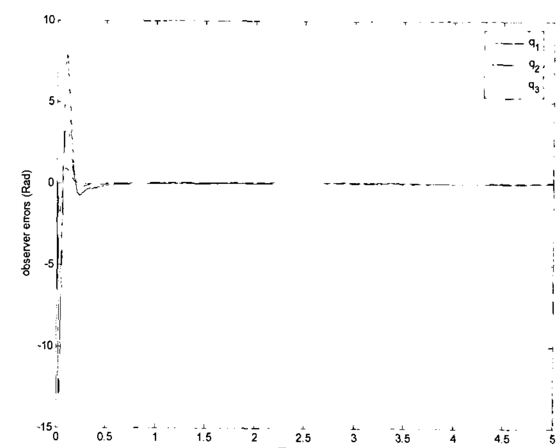

(b) State $\mathbf{x}_4$.

Fig. 3. Observation errors for the three-link FJ manipulator.

The control objective is to design the output feedback control law $\mathbf{u}$ using only position measurements to track the reference trajectory $\mathbf{q_d} = [q_{d1}\ q_{d2}\ q_{d3}]^T$ as follows:

$$q_{d1} = 1 + 0.5cos(1.5t + \frac{\pi}{3}),$$

$$q_{d2} = 0.7sin(1.5t + \frac{2\pi}{3}),$$

$$q_{d3} = 1 + 0.3cos(1.5t).$$

The matrices $\mathbf{M}(\mathbf{q})$, $\mathbf{C}(\mathbf{q},\dot{\mathbf{q}})$, $\mathbf{G}(\mathbf{q})$, and system parameters of the three-link FJ manipulator are defined in Appendix II. In Appendix II, m_i s are the link masses (kg); a_i s are the link lengths (m); I_{oi} s are the moment of inertia about the center of gravity (Kgm^2); g is the acceleration of gravity; q_i s are the joint angular positions (rad); S_{ij} and C_{ij} denote $\sin(q_i + q_j)$ and $\cos(q_i + q_j)$, respectively. And, the FJ parameters are chosen as $\mathbf{J} = \text{diag}[0.5\ \ 0.5\ \ 0.5]$,

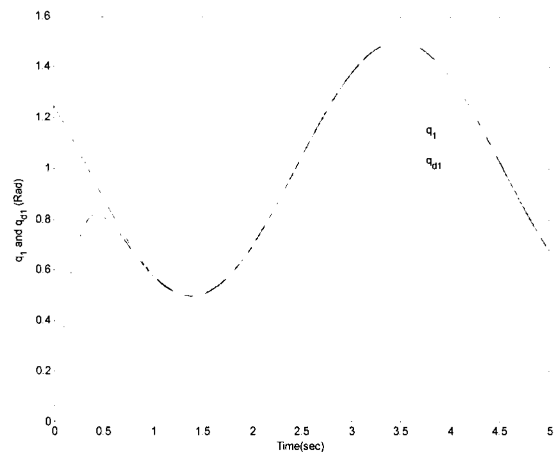

(a) Joint 1.

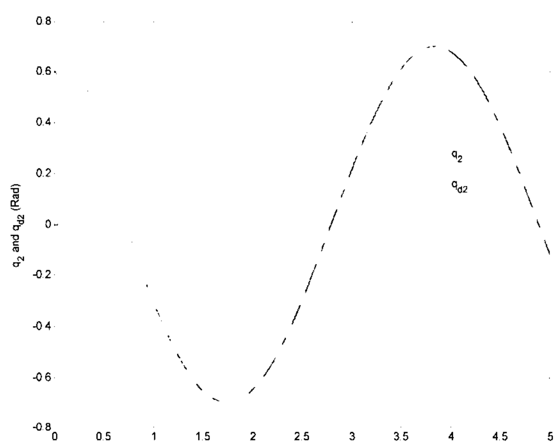

(b) Joint 2.

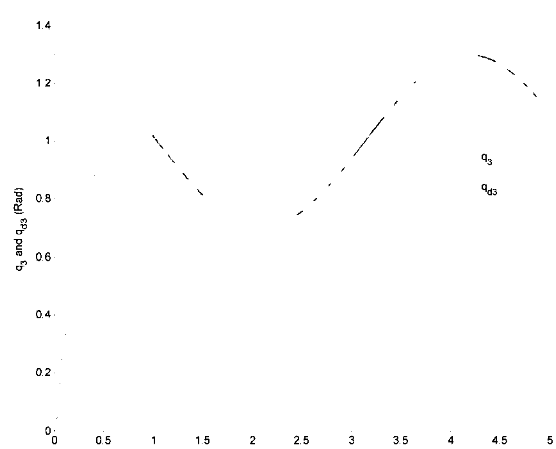

(c) Joint 3.

Fig. 4. Tracking results for the three-link FJ manipulator.

$\mathbf{B} = \text{diag}[0.02\ 0.02\ 0.02]$, and $\mathbf{K_m} = \text{diag}[15\ 15\ 15]$. In this simulation, the initial positions of the three-link FJ manipulator are also set to $q_1(0) = q_2(0) = q_3(0)$ and the observer and controller parameters for the OFDSC system are selected as $l_1 = 25$, $l_2 = 20$, $\mathbf{D}_1 = \mathbf{D}_3 = 5\mathbf{I}$, $\mathbf{D}_2 = \mathbf{D}_4 = \mathbf{I}$, $k_1 = 130$, $k_2 = 15$, $k_3 = 5$, $k_4 = 120$, and $\tau_2 = \tau_3 = \tau_4 = 0.001$. The observation results of the states $\mathbf{x}_2$ and $\mathbf{x}_4$ are displayed in Figs. 1 and 2, respectively. Fig. 3 shows the observation errors of the link and actuator velocities for the OFDSC system. From these figures, note that the proposed method demonstrates the good observation performance. The tracking results and errors of the OFDSC system are shown in Figs. 4 and 5. These figures indicate that the tracking errors which occur at the starting point drop quickly in less than a few seconds. Besides, we can see that all signals in the closed-loop system are bounded.

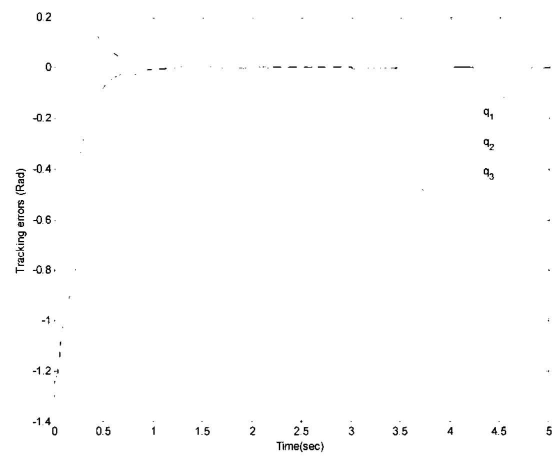

Fig. 5. Tracking errors for the three-link FJ manipulator.

5. CONCLUSION

A new output feedback control design method for the FJ robot has been developed based on observer DSC technique. First, the dynamics of the FJ robots has been introduced. Second, an observer for FJ robots has been presented to estimate the link and actuator velocity information, and it has been used to design the simple OFDSC law for the tracking control of the FJ robots. Third, from Lyapunov stability analysis, it has been shown that all signals in the closed-loop system are uniformly ultimately bounded. Finally, we have presented the simulation results for the three-link FJ manipulator to verify the effectiveness of the proposed OFDSC approach.

APPENDIX I

Proof of Theorem 1: Let us consider the following Lyapunov candidate function:

$$V = V_c + V_o, \tag{52}$$

$$V_c = \frac{1}{2}\left[\sum_{l=1}^{4} \mathbf{S}_l^T \mathbf{S}_l + \sum_{l=1}^{3} \mathbf{y}_{l+1}^T \mathbf{y}_{l+1}\right], \tag{53}$$

$$V_o = \frac{1}{2}[\tilde{\mathbf{x}}_1^{\mathbf{T}}\tilde{\mathbf{x}}_1 + \tilde{\mathbf{x}}_2^{\mathbf{T}}\mathbf{M}(\mathbf{x}_1)\tilde{\mathbf{x}}_2 + \tilde{\mathbf{x}}_3^{\mathbf{T}}\tilde{\mathbf{x}}_3 + \tilde{\mathbf{x}}_4^{\mathbf{T}}\tilde{\mathbf{x}}_4. \tag{54}$$

For the stability analysis of the total system, we first consider the Lyapunov candidate function V_c for the controller. Differentiating (53) with respect to time and substituting (45)-(51), we can obtain

$$\begin{aligned}\dot{V}_c &= \mathbf{S}_1^T(\mathbf{S}_2+\mathbf{y}_2-k_1\mathbf{S}_1+\tilde{\mathbf{x}}_2)\\&+\mathbf{S}_2^T(\mathbf{M}^{-1}(\mathbf{x}_1)\mathbf{K_m}(\mathbf{S}_3+\mathbf{y}_3)-k_2\mathbf{S}_2+l_1\tilde{\mathbf{x}}_2)\\&+\mathbf{S}_3^T(\mathbf{S}_4+\mathbf{y}_4-k_3\mathbf{S}_3+\tilde{\mathbf{x}}_4)+\mathbf{S}_4^T(-k_4\mathbf{S}_4+l_2\tilde{\mathbf{x}}_4)\\&+\sum_{l=1}^{3}\mathbf{y}_{l+1}^T\left(-\frac{\mathbf{y}_{l+1}}{\tau_{l+1}}+\Omega_{l+1}\right)\\&\le\|\mathbf{S}_1\|\|\mathbf{S}_2\|+\|\mathbf{S}_1\|\|\mathbf{y}_2\|+\|\mathbf{S}_1\|\|\tilde{\mathbf{x}}_2\|-\sum_{l=1}^{4}k_l\|\mathbf{S}_l\|^2\\&+\left\|\mathbf{M}^{-1}(\mathbf{x}_1)\mathbf{K_m}\right\|_2\|\mathbf{S}_2\|\|\mathbf{S}_3\|+l_1\|\mathbf{S}_2\|\|\tilde{\mathbf{x}}_2\|\\&+\left\|\mathbf{M}^{-1}(\mathbf{x}_1)\mathbf{K_m}\right\|_2\|\mathbf{S}_2\|\|\mathbf{y}_3\|+\|\mathbf{S}_3\|\|\mathbf{S}_4\|\\&+\|\mathbf{S}_3\|\|\mathbf{y}_4\|+\|\mathbf{S}_3\|\|\tilde{\mathbf{x}}_4\|+l_2\|\mathbf{S}_4\|\|\tilde{\mathbf{x}}_4\|\\&+\sum_{l=1}^{3}\left(-\frac{1}{\tau_{l+1}}\|\mathbf{y}_{l+1}\|^2+\|\mathbf{y}_{l+1}\|\|\Omega_{l+1}\|\right).\end{aligned}$$

By applying Property 4 and Young's Inequality, we obtain

$$\begin{aligned}\dot{V}_c &\le\|\mathbf{S}_1\|^2+\frac{1}{4}\|\mathbf{S}_2\|^2+\|\mathbf{S}_1\|^2+\frac{1}{4}\|\mathbf{y}_2\|^2+\|\mathbf{S}_1\|^2\\&+\frac{1}{4}\|\tilde{\mathbf{x}}_2\|^2+H_M\left(\|\mathbf{S}_2\|^2+\frac{1}{4}\|\mathbf{S}_3\|^2\right)\\&+H_M\left(\|\mathbf{S}_2\|^2+\frac{1}{4}\|\mathbf{y}_3\|^2\right)+l_1\left(\|\mathbf{S}_2\|^2+\frac{1}{4}\|\tilde{\mathbf{x}}_2\|^2\right)\\&+\|\mathbf{S}_3\|^2+\frac{1}{4}\|\mathbf{S}_4\|^2+\|\mathbf{S}_3\|^2+\frac{1}{4}\|\mathbf{y}_4\|^2+\|\mathbf{S}_3\|^2+\frac{1}{4}\|\tilde{\mathbf{x}}_4\|^2\\&+l_2\left(\|\mathbf{S}_4\|^2+\frac{1}{4}\|\tilde{\mathbf{x}}_4\|^2\right)-\sum_{l=1}^{4}k_l\|\mathbf{S}_l\|^2\\&+\sum_{l=1}^{3}\left(-\frac{1}{\tau_{l+1}}\|\mathbf{y}_{l+1}\|^2+\|\mathbf{y}_{l+1}\|^2+\frac{1}{4}\|\Omega_{l+1}\|^2\right).\end{aligned}$$

Choosing $k_1=k_1^*+3$, $k_2=k_2^*+2H_M+l_1+(1/4)$, $k_3=k_3^*+(H_M/4)+3$, $k_4=k_4^*+(1/4)+l_2$, $1/\tau_2=\gamma_2+(5/4)$, $1/\tau_3=\gamma_3+(H_M/4)+1$, and $1/\tau_4=\gamma_4+(5/4)$ yields

$$\begin{aligned}\dot{V}_c &\le-\sum_{l=1}^{4}k_l^*\|\mathbf{S}_l\|^2-\sum_{l=1}^{3}\gamma_{l+1}\|\mathbf{y}_{l+1}\|^2+\frac{1}{4}(1+l_1)\|\tilde{\mathbf{x}}_2\|^2\\&+\frac{1}{4}(1+l_2)\|\tilde{\mathbf{x}}_4\|^2+\sum_{l=1}^{3}\frac{1}{4}\|\Omega_{l+1}\|^2,\end{aligned}\quad(55)$$

where $k_l^*>0$, $\gamma_{l+1}>0$ are design parameters. Then, let us consider the Lyapunov candidate function V_o. The derivative of V_o using (33), (35)-(37), and Property 2 can be obtained as follows:

$$\begin{aligned}\dot{V}_o &= \tilde{\mathbf{x}}_1^T\tilde{\mathbf{x}}_2-\tilde{\mathbf{x}}_1^T\mathbf{D}_1\tilde{\mathbf{x}}_1-\tilde{\mathbf{x}}_2^T\mathbf{C}(\mathbf{x}_1,\hat{\mathbf{x}}_2)\tilde{\mathbf{x}}_2-\tilde{\mathbf{x}}_2^T\mathbf{F}\tilde{\mathbf{x}}_2\\&-l_1\tilde{\mathbf{x}}_2^T\mathbf{M}(\mathbf{x}_1)\tilde{\mathbf{x}}_2-\tilde{\mathbf{x}}_2^T\mathbf{D}_2\tilde{\mathbf{x}}_1+\tilde{\mathbf{x}}_3^T\tilde{\mathbf{x}}_4-\tilde{\mathbf{x}}_3^T\mathbf{D}_3\tilde{\mathbf{x}}_3\\&-\tilde{\mathbf{x}}_4^T\mathbf{J}^{-1}\mathbf{B}\tilde{\mathbf{x}}_4-l_2\tilde{\mathbf{x}}_4^T\tilde{\mathbf{x}}_4-\tilde{\mathbf{x}}_4^T\mathbf{D}_4\tilde{\mathbf{x}}_3.\end{aligned}$$

Here, choosing $\mathbf{D}_1=d_1\mathbf{I}$, $\mathbf{D}_3=d_3\mathbf{I}$, and $\mathbf{D}_2=\mathbf{D}_4=\mathbf{I}$, we obtain

$$\begin{aligned}\dot{V}_o &\le-d_1\tilde{\mathbf{x}}_1^T\tilde{\mathbf{x}}_1-\tilde{\mathbf{x}}_2^T(\mathbf{C}(\mathbf{x}_1,\hat{\mathbf{x}}_2)+\mathbf{F}+l_1\mathbf{M}(\mathbf{x}_1))\tilde{\mathbf{x}}_2\\&-d_3\tilde{\mathbf{x}}_3^T\tilde{\mathbf{x}}_3-l_2\tilde{\mathbf{x}}_4^T\tilde{\mathbf{x}}_4,\end{aligned}$$

where d_1 and d_3 denote the positive constants, $\mathbf{I}\in R^{n\times n}$ is an identity matrix. Using Properties 1 and 3, and Assumption 3, the term $\tilde{\mathbf{x}}_2^T(\mathbf{C}(\mathbf{x}_1,\hat{\mathbf{x}}_2)+\mathbf{F}+l_1\mathbf{M}(\mathbf{x}_1))\tilde{\mathbf{x}}_2$ can be represented by

$$\begin{aligned}&\tilde{\mathbf{x}}_2^T(\mathbf{C}(\mathbf{x}_1,\hat{\mathbf{x}}_2)+\mathbf{F}+l_1\mathbf{M}(\mathbf{x}_1))\tilde{\mathbf{x}}_2\\&\quad\ge[l_1M_m-f_m-C_M(\omega_1+\omega_2)]\tilde{\mathbf{x}}_2^T\tilde{\mathbf{x}}_2,\end{aligned}$$

where ω_2 is the upper bound of the initial observation error $\tilde{\mathbf{x}}_2$, and f_m denotes the minimum eigenvalue of the matrix **F**. Therefore, using Young's Inequality, we obtain

$$\begin{aligned}\dot{V}_o &\le-d_1\|\tilde{\mathbf{x}}_1\|^2-\beta_1\|\tilde{\mathbf{x}}_2\|^2-d_3\|\tilde{\mathbf{x}}_3\|^2\\&-l_2\|\tilde{\mathbf{x}}_4\|^2+\|\tilde{\mathbf{x}}_2\|^2+\|\tilde{\mathbf{x}}_4\|^2,\end{aligned}\quad(56)$$

where $\beta_1=l_1M_m-f_m-C_M(\omega_1+\omega_2)$. Finally, we consider the total Lyapunov candidate function V. By adding (55) and (56), the derivative of the total Lyapunov candidate function V can be obtained as follows:

$$\begin{aligned}\dot{V}&=\dot{V}_c+\dot{V}_o\\&\le-\sum_{l=1}^{4}k_l^*\|\mathbf{S}_l\|^2-\sum_{l=1}^{3}\gamma_{l+1}\|\mathbf{y}_{l+1}\|^2-d_1\|\tilde{\mathbf{x}}_1\|^2\\&-\beta_1\|\tilde{\mathbf{x}}_2\|^2-d_3\|\tilde{\mathbf{x}}_3\|^2-l_2\|\tilde{\mathbf{x}}_4\|^2+\frac{1}{4}(5+l_1)\|\tilde{\mathbf{x}}_2\|^2\\&+\frac{1}{4}(5+l_2)\|\tilde{\mathbf{x}}_4\|^2+\sum_{l=1}^{3}\frac{1}{4}\|\Omega_{l+1}\|^2.\end{aligned}$$

From Assumption 2, and the existence of p, there exist a positive constant δ_{l+1} such that $\|\Omega_{l+1}\|\le\delta_{l+1}$. Therefore, by choosing $l_1=[d_2+f_m+C_M$

$(\omega_1+\omega_2)+(5/4)]/[M_m-(1/4)]$, $l_2=(4/3)d_4+(5/3)$, we obtain

$$\begin{aligned}\dot V &\le -\sum_{l=1}^{4} k_l^* \|\mathbf{S}_l\|^2 - \sum_{l=1}^{4} d_l \|\tilde{\mathbf{x}}_l\|^2 - \sum_{l=1}^{3} \gamma_{l+1}\|\mathbf{y}_{l+1}\|^2 + C \\ &\le -2\varpi V + C, \end{aligned} \qquad (57)$$

where d_2 and d_4 are the positive constants, $C=\sum_{l=1}^{3}\frac{1}{4}\delta_{l+1}^2$, and $0<\varpi<\min[k_1^*,\ldots,k_4^*,d_1,\frac{d_2}{M_M},d_3,d_4,\gamma_2,\gamma_3,\gamma_4]$. (6) implies $\dot V\le 0$ on $V=p$ when $\varpi>(C/2p)$. Therefore $V\le p$ is an invariant set, i.e. if $V(0)\le p$, then $V(t)\le p$ for all $t\ge 0$. In addition, all error signals in the closed-loop system are uniformly ultimately bounded in the following compact set Ξ:

$$\Xi=\left\{\mathbf{S}_1,\ldots,\mathbf{S}_4,\tilde{\mathbf{x}}_1,\ldots,\tilde{\mathbf{x}}_4,\mathbf{y}_1,\mathbf{y}_2,\mathbf{y}_3 \,\middle|\, \sum_{l=1}^{4}\|\mathbf{S}_l\|^2+\|\tilde{\mathbf{x}}_1\|^2 + M_m\|\tilde{\mathbf{x}}_2\|^2+\|\tilde{\mathbf{x}}_3\|^2+\|\tilde{\mathbf{x}}_4\|^2+\gamma_{l+1}\|\mathbf{y}_{l+1}\|^2\le\frac{C}{\varpi}\right\}.$$

Besides, the compact set Ξ can be kept arbitrarily small by adjusting k_l^*, d_l, γ_j, where $l=1,\ldots,4$, and $j=2,3,4$. That is, the tracking error $\mathbf{S}_1$ and the observation errors $\tilde{\mathbf{x}}_2$, $\tilde{\mathbf{x}}_4$ can be made arbitrarily small. This completes the proof of Theorem 1.

APPENDIX II

The matrices $\mathbf{M}(\mathbf{q})$, $\mathbf{C}(\mathbf{q},\dot{\mathbf{q}})$, and $\mathbf{G}(\mathbf{q})$ of robot dynamics are as follows:

$$\mathbf{M}(\mathbf{q})=\begin{bmatrix} 2d_1+d_4C_2+d_5C_{23} & 2d_2+d_4C_2+d_6C_3 & 2d_5+d_5C_{23}+d_6C_3 \\ d_4C_2+d_5C_{23} & 2d_2+d_6C_3 & 2d_3+d_6C_3 \\ d_5C_{23} & d_6C_3 & 2d_3 \end{bmatrix}\begin{bmatrix}1&0&0\\1&1&0\\1&1&1\end{bmatrix},$$

$$\mathbf{C}(\mathbf{q},\dot{\mathbf{q}})=\begin{bmatrix} C_{m11} & C_{m12} & C_{m13} \\ C_{m21} & C_{m22} & C_{m23} \\ C_{m31} & C_{m32} & C_{m33}\end{bmatrix},$$

$$\mathbf{G}(\mathbf{q})=\begin{bmatrix} \frac{1}{2}a_1C_1 & a_1C_1+\frac{1}{2}a_2C_{12} & a_1C_1+a_2C_{12}+\frac{1}{2}a_3C_{123} \\ 0 & \frac{1}{2}a_2C_{12} & a_2C_{12}+\frac{1}{2}2a_3C_{123} \\ 0 & 0 & \frac{1}{2}a_3C_{123} \end{bmatrix}\begin{bmatrix} m_1g \\ m_2g \\ m_3g \end{bmatrix},$$

where

$$\begin{aligned}
C_{m11}&=-\dot q_2d_4S_2-\dot q_2d_5S_{23}-\dot q_3d_5S_{23}-\dot q_3d_6S_3,\\
C_{m12}&=-\dot q_2d_4S_2-\dot q_2d_5S_{23}-\dot q_3d_6S_3-\dot q_3d_5S_{23}\\
&\quad -\dot q_1d_4S_2-\dot q_1d_5S_{23},\\
C_{m13}&=-\dot q_2d_5S_{23}-\dot q_3d_5S_{23}-\dot q_3d_6S_3-\dot q_1d_5S_{23}\\
&\quad -\dot q_1d_6S_3-\dot q_2d_6S_3,\\
C_{m21}&=-\dot q_3d_6S_3+\dot q_1d_4S_2+\dot q_1d_5S_{23},\\
C_{m22}&=-\dot q_3d_6S_3,\\
C_{m23}&=-d_6S_3(\dot q_1+\dot q_2+\dot q_3),\\
C_{m31}&=\dot q_1d_5S_{23}+\dot q_1d_6S_3+\dot q_2d_6S_3,\\
C_{m32}&=d_6S_3(\dot q_1+\dot q_2),\\
C_{m33}&=0,
\end{aligned}$$

and

$$\begin{aligned}
d_1&=\frac{1}{2}[(\frac{1}{4}m_1+m_2+m_3)a_1^2+I_{o1}],\\
d_2&=\frac{1}{2}[(\frac{1}{4}m_2+m_3)a_2^2+I_{o2}],\\
d_3&=\frac{1}{2}[(\frac{1}{4}m_3)a_3^2+I_{o3}],\\
d_4&=(\frac{1}{2}m_2+m_3)a_1a_2,\\
d_5&=\frac{1}{2}m_3a_1a_3,\\
d_6&=\frac{1}{2}m_3a_2a_3.
\end{aligned}$$

REFERENCES

[1] J. H. Oh and J. S. Lee, “Control of flexble joint robot system by backstepping design approach,” *Proc. of the IEEE Int. Conf. Robotics and Automation*, pp. 3435-3429, 1997.

[2] A. A. Abouelsoud, “Robust regulator for flexible-joint robots using integrator backstepping,” *Journal of Intelligent and Robotic Systems*, vol. 22, pp. 23-38, 1998.

[3] S. Nicosia and P. Tomei, “A new approach to control elastic joint robots with application to adaptive control,” *Proc. of IEEE Conf. Decision and Control*, pp. 343-347, 1991.

[4] C. W. Park and Y. W. Cho, “Adaptive tracking control of flexible joint manipulator based on

fuzzy model reference approach," *IEE Proc. Control Theory and Appl.*, vol. 150, no. 2, pp. 198-204, 1992.

[5] E. Gurkan, S. P. Banks, and I. Erkmen, "Stable controller design for the T-S fuzzy model of a flexible-joint robot arm based on Lie algebra," *Proc. of IEEE Conf. Decision and Control*, pp. 4717-4722, 2003.

[6] C. J. B. Macnab, G. M. T. D'Eleuterio and M. Meng, "CMAC adaptive control of flexible-joint robots using backstepping with tuning functions," *Proc. of the IEEE Int. Conf. Robotics and Automation*, pp. 2679-2686, 2004.

[7] C. Kwan and F. L. Lewis, "Robust backstepping control of nonlinear systems using neural networks," *IEEE Trans. on Systems, Man, and Cybernetics, Part A: Syst. Humans*, vol. 30, no. 6, pp. 753-766, 2000.

[8] P. Tomei, "An observer for flexible joint robots," *IEEE Trans. on Automatic Control*, vol. 35, no. 6, pp. 739-743, 1990.

[9] E. Gyurkovics and D. Svirko, "A nonlinear observer for flexible joint robots," *Periodica Polytechnica Ser. Mech. Eng.*, vol. 46, no. 2, pp. 127-137, 2002.

[10] F. Abdollahi, H. A. Talebi, and R. V. Patel, "A stable neural network-based observer with application to flexible-joint manipulators," *IEEE Trans. on Neural Networks*, vol. 17, no. 1, pp. 118-129, 2006.

[11] J. D. León-morales, J. G. Alvarez-leal, R. Castro-linares, and J. Alvarez-gallegos, "Control of a flexible joint manipulator via a non-linear control-observer scheme," *International Journal of Control*, vol. 74, no. 3, pp. 290-302, 2001.

[12] A. R. Angeles and H. Nijmeijer, "Synchronizing tracking control for flexible joint robots via estimated state feedback," *Journal of Dynamic Systems, Measurement, and Control*, vol. 126, pp. 162-172, 2004.

[13] M. Jankovic, "Observer based control for elastic joint robots," *IEEE Trans. on Robotics and Automation*, vol. 11, no. 4, pp. 618-623, 1995.

[14] M. Krstic, I. Kanellakopoulos, and P. Kokotovic, *Nonlinear and Adaptive Control Design*, Wiley Interscience, NJ, 1995.

[15] S. Nicosia and P. Tomei, "A global output feedback controller for flexible joint robots," *Automatica*, vol. 31, no. 10, pp. 1465-1469, 1995.

[16] S. Nicosia and P. Tomei, "A Tracking controller for flexible joint robots using only link position feedback," *IEEE Trans. on Automatic Control*, vol. 40, no. 5, pp. 885-890, 1995.

[17] J. H. Oh and J. S. Lee, "Backstepping control design of flexible joint manipulator using only position measurements," *Proc. of the IEEE Conf. Decision and Control*, pp. 931-936, 1998.

[18] S. Y. Lim, D. M. Dawson, J. Hu, and M. S. D. Queiroz, "An adaptive link position tracking controller for rigid-link flexible-joint robots without velocity measurements," *IEEE Trans. on Systems, Man, and Cybernetics*, vol. 27, no. 3, pp. 412-427, 1997.

[19] W. E. Dixon, E. Zergeroglu, D. M. Dawson, and M. W. Hannan, "Global adaptive partial state feedback tracking control of rigid-link flexible-joint robots," *Robotica*, vol. 18, pp. 325-336, 2000.

[20] D. Swaroop, J. K. Hedrick, P. P. Yip, and J. C. Gerdes, "Dynamic surface control for a class of nonlinear systems," *IEEE Trans. on Automatic Control*, vol. 45, no. 10, pp. 1893-1899, 2000.

[21] P. P Yip and J. K. Hedrick, "Adaptive dynamic surface control: A simplified algorithm for adaptive backstepping control of nonlinear systems," *Int. Jour. of Control*, vol. 71, no. 5, pp 959-979, 1998.

[22] D. Wang and J. Huang, "Neural network-based adaptive dynamic surface control for a class of uncertain nonlinear systems in strict-feedback form," *IEEE Trans. on Neural Networks*, vol. 16, no. 1, pp. 195-202, 2005.

[23] B. Song and J. K. Hedrick, "Observer-based dynamic surface control for a class of nonlinear systems: An LMI Approach," *IEEE Trans. on Automatic Control*, vol. 49, no. 11, pp. 1995-2001, 2004.

[24] S. J. Yoo, J. B. Park, and Y. H. Choi, "Adaptive dynamic surface control of flexible-joint robots using self-recurrent wavelet neural networks," *IEEE Trans. on Systems, Man, and Cybernetics, Part B: Cybernetics*, vol. 36, no. 6, pp. 1342-1355, 2006.

[25] M. W. Spong, "Adaptive control of flexible-joint manipulators," *System Control Letters*, vol. 13, pp. 15-21, 1989.

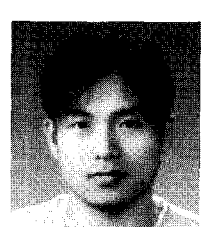

Sung Jin Yoo received the B.S. and M.S. degrees from Yonsei University, Seoul, Korea, in 2003 and 2005, respectively, both in Electrical and Electronic Engineering. He is currently working toward a Ph.D. degree at Yonsei University. His research interests include nonlinear, robust, adaptive control, and neural networks theories, and their applications to robotic, flight, and chaos systems.

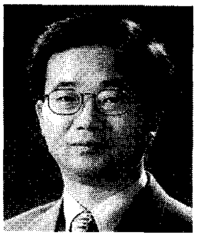

Jin Bae Park received the B.S. degree in Electrical Engineering from Yonsei University, Seoul, Korea, in 1977 and the M.S. and Ph.D. degrees in Electrical Engineering from Kansas State University, Manhattan, in 1985 and 1990, respectively. Since 1992 he has been with the Department of Electrical and Electronic Engineering, Yonsei University, Seoul, Korea, where he is currently a Professor. His research interests include robust control and filtering, nonlinear control, mobile robot, fuzzy logic control, neural networks, and genetic algorithms. He had served as Vice-President for the Institute of Control, Automation and Systems Engineers. He currently serves as Editor-in-Chief for the *International Journal of Control, Automation, and Systems*.

Yoon Ho Choi received the B.S., M.S., and Ph.D. degrees in Electrical Engineering from Yonsei University, Seoul, in 1980, 1982 and 1991, respectively. Since 1993, he has been with School of Electronic Engineering at Kyonggi University, where he is currently a Professor. From 2000 to 2002, he was with the Department of Electrical Engineering, Ohio State University, where he was a Visiting Scholar. His research interests include nonlinear control theory, intelligent control, biped and mobile robots, web-based control system and wavelet transform. He is currently the Director for the Institute of Control, Robotics and Systems.